Polish Society of Composite Materials
Polskie Towarzystwo Materiałów Kompozytowych

21: 3 (2021) 61-69

COMPOSITES THEORY AND PRACTICE
ISSN: 2084-6096
ISSN (online): 2299-128X

Mohammad Afzali*, Vahid Asghari

Islamic Azad University, Department of Mechanical Engineering, Sari Branch, Sari, Iran
**Corresponding author: E-mail: mohammad2142.ma@gmail.com*

Received (Otrzymano) 2.03.2021

ANALYZING MECHANICAL BEHAVIOR OF ABS-SiO_2 POLYMER-BASED NANOCOMPOSITE BASED ON ANOVA METHOD

The fabrication of polymer-based nanocomposites by means of twin extruders is a typical method for manufacturing lightweight and high-strength structures. However, selection of the optimal parameters for this process to study the material characteristics is important. The primary aim of the present study was to ascertain the optimum extruder temperature and nanosilica content in an acrylonitrile-butadiene-styrene matrix composite. The response surface methodology was based on two factors and three levels. The identification of the effect of the parameters on the fatigue behavior of the fabricated composite was comprehensively analyzed. The results were analyzed using scanning electron microscopy (SEM). The obtained results revealed that up to 4% nano-SiO_2 improves tensile strength and reduces the impact toughness. On the other hand, an increase in the extrusion temperature yields a higher impact toughness and lower tensile strength. The optimization results showed that 2.5% nanosilica and the extrusion temperature of 225°C result in the maximum tensile strength of 41 MPa, and impact toughness of 30 KJ/m^2.

Keywords: acrylonitrile-butadiene-styrene, nano-silica, extrusion, RSM, tensile strength, impact toughness, fatigue behavior

INTRODUCTION

Acrylonitrile-butadiene-styrene (ABS) is usually used commercially due to its desirable physical properties and low cost of fabrication. The main applications of the ABS polymer are automobile parts, household items, and electrical housing, among others. The main advantages of the ABS polymer are good strain resistance, impact resistance even at low temperatures, good abrasion resistance, tough and stiffness. However, this material faces some problems such as low common mechanical properties including ultimate strength and hardness [1]. For these reasons, researchers focused on enhancing the mechanical properties by reinforcing with nanoceramic materials to produce a polymer matrix nanocomposite [2, 3].

Several nanoparticles are needed to prepare a polymer nanocomposite. Limited work has been done on different nanoparticles like clay, MMT, mica, talc, alumina, and others in ABS polymeric systems. There are still only a few reports on the preparation of ABS nanocomposites, and several works have been done on alumina nanoparticles in ABS polymeric systems.

Jang et al. [4] reported on the fabrication of an ABS-based nanocomposite reinforced by clay by the emulsion technique. Wang et al. [5] also studied the characterization of a delaminated nanocomposite by direct melt intercalation. Stretz et al. [6], found that by dispersing of clay particles in styrene-acrylonitrile polymer-based nanocomposite (SAN), accumulation was observed. Pourabas and Raeesi [7] prepared an ABS/clay nanocomposite using a solvent/non-solvent method and adopting different mixing methods. In another attempt, Jang and Wilkie [8] studied the effect of clay on the thermal degradation behavior of ABS. They found that the addition of a nanoceramic material significantly improves the performance mentioned above. Modesti et al. [9] investigated the effect of a clay surfactant on the morphology of the developed composite. Tenget et al. [10] studied the effect of particle size in an alumina-based nanocomposite. They ascertained that the role of the particles in the microstructure and the fatigue behavior is significant. They found that the fracture mode of the manufactured composite changes to intergranular, and the strength increases considerably. Kuo et al. [11] investigated the effect of nano-sized alumina on the mechanical and thermal stability of the PEEK nanocomposite and found that both properties improved with an increase in the nanoalumina content.

In the fabrication of a polymer matrix nanocomposite, silica (SiO_2) nanoparticles is one of the most widely used reinforcements. Different researchers have used it to enhance fatigue behavior, thermal stability, and surface properties. Lin et al. [12] reported that nano-SiO_2 is beneficial in improving the bonding strength of the UF adhesive and reducing its free formaldehyde emissions. Devi and Maji [13] studied the fabrication of wood polymer nanocomposites (WPNC)

based on nano-SiO_2. They reported that the fatigue behavior, water uptake, and thermal stability improve by adding SiO_2 particles to the wood/polymer matrix. Hsu and Lin [14] used different types of catalysts to prepare a composite material. It was reported that the ABS/SiO_2 composite, which was fabricated by using NH_4F as the catalyst material has higher strength, a more delicate structure, and a smoother surface. With comparing to those composites prepared by the HCl catalyzer. Zheng et al. [3] studied the synthesis of silica-graft acrylonitrile-butadiene-styrene nanocomposites. The silica-graft ABS composites were prepared by an open ring reaction and radical grafting copolymerization of modified silica, styrene, and maleic anhydride (MAH) in an ABS/THF solution. The differential scanning calorimetry (DSC) results show that the glass transition temperature (T_g) of silica-graft ABS composites shifts to higher temperatures with an increasing silica content.

Nonetheless, the optimization of the twin extrusion process involving multiple factors and multiple responses has hardly been reported in the literature. Hence, this article deals with the application of RSM in developing empirical relationships relating essential input variables, namely the nanosilica content (W) and extrusion temperature (T), to the fatigue behavior of the ABS-SiO_2 polymer matrix nanocomposite. Furthermore, this article illustrates how some overlapping response surfaces can be used to select the operating conditions necessary to achieve the desired specifications and optimize the process.

The range of the selected parameters and the conclusions refer specifically to the physical nature of the process and the cross-section in this study. Nevertheless, the illustrated approach and the response surface methodology are universal.

MATERIALS AND METHOD

Materials

The matrix material chosen for this study was the ABS polymer (Absolac-920 Bayer), a high flow, medium impact grade. Table 1 shows the physical and fatigue behavior of ABS.

TABLE 1. **Physical and fatigue behavior of ABS**

Properties	Value
Tensile strength [MPa]	6.8
Notched impact strength [kJ/m^2]	3-30
Thermal coefficient of expansion	100-150×10^{-6}
Melting point (centigrade)	160
Density [g/cm^3]	0.905

Nano-sized silica particles obtained from NOTRONO CO. (IRAN) were used as the reinforcement material with an average particle diameter of 50 nm, density of 3.97 g/cm^3, and a 2050ºC melting point. It should be noted that the silica particles are added in a lower amount in volume than conventional polymeric composites. This means that the current nanocomposites would not alter much the processability or density of the ABS matrix.

Compounding and sampling

The composite samples for tensile and impact tests were prepared by first mixing pre-weighed quantities of ABS graduals and nanoalumina powder of different volumes (0-5%), followed by manual melt mixing in a double screw extruder (BRABENDER 6300) 18 mm with an L/D ratio of 24/1. During the process, the melt temperature varied between 180 to 240ºC. The screw speed was kept constant at 60 RPM for all the compositions.

To improve the mixing of the materials, the raw ABS was dried at 60ºC in a vacuum oven for at least 12 h to remove moisture and impurities. The nanosilica was also dried at 90ºC for 10 hours to prevent water uptake. Continuous mixing was performed during extrusion, and the extrusions were cooled by water at the exit of the die and then air-cooled; after cooling, the composite rods were cut into a uniform size by a Pelletizer machine.

The injection molding process prepared the nanocomposite samples for mechanical characterization. The tensile test samples and impact test samples were formed using specified dies according to required standard sizes. Figure 1 presents the extrusion machine and the extruded samples for the tensile and Charpy impact test tests.

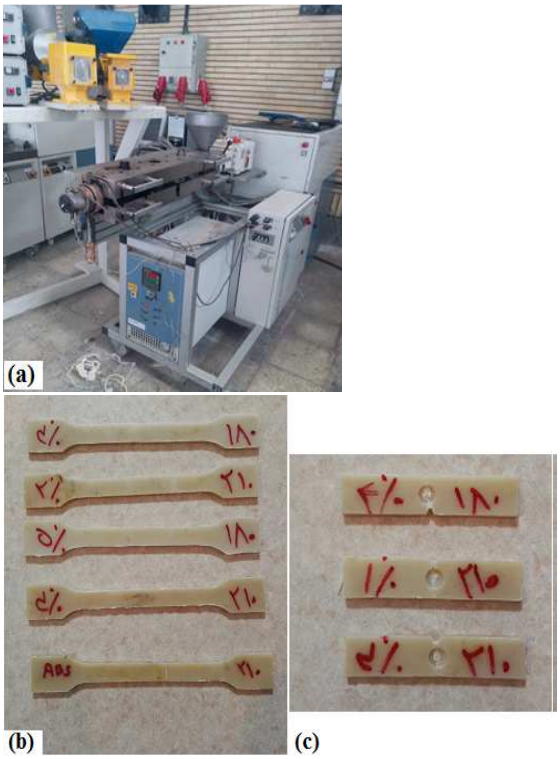

Fig. 1. Extrusion machine (a), prepared samples for tensile tests (b), prepared samples for impact tests (c)

Morphology analysis

Scanning electron microscopy was used to determine the dispersion morphology of the alumina particles in the ABS polymer matrix. The morphology of the developed nanocomposite was analyzed using the obtained SEM micrographs at 20 kV. The scanning electron microscope Cam Scan MV2300 was used to study the morphology of the ABS/silica nanocomposite. Figure 2a shows the SEM used for the observations.

Mechanical testing

The tensile and impact tests were carried out on a universal testing machine (SANTAM 30T) and an E310 Charpy impact testing machine (SANTAM). The samples were prepared according to the ASTM-D3039M - 17 and ASTM D6110 - 18 standards for tensile strength and Charpy impact tests. For the tensile tests, the span length was 100 mm, and the crosshead speed was 5 mm/min. Figure 2b-c present the test machines for the tensile and impact tests, respectively.

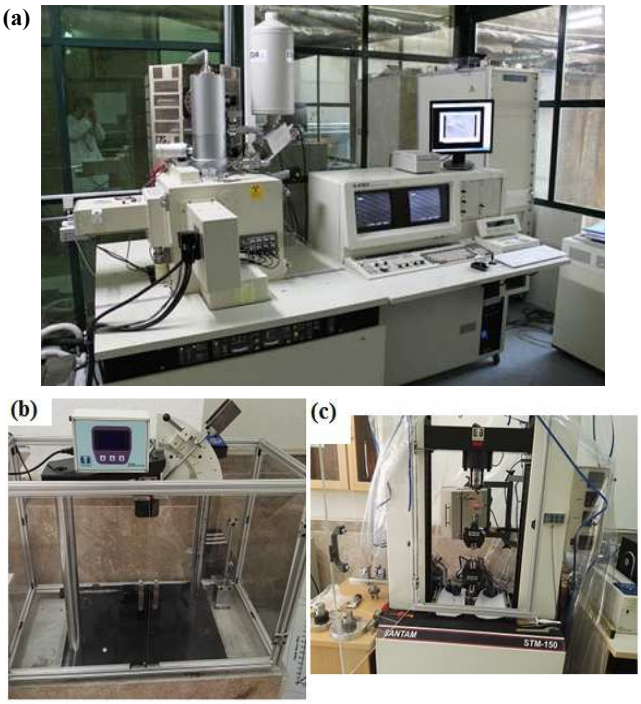

Fig. 2. Devices for characterization and testing: a) SEM, b) Charpy test for impact testing, c) universal testing machine for tensile testing

Research methodology

Three factors and three levels of central composite design were employed to study the effect of the silica content and extrusion temperature. According to this type of design, 13 experiments should be carried out. Table 2 presents the design matrix and values of responses that were measured after the experiments. Each experiment was conducted three times to avoid stochastic results, and the average values of the tensile strength and impact energy were reported.

TABLE 2. **Design matrix and observed values of composite strength**

No	SiO_2 content [%]	Temperature [°C]	Tensile strength [MPa]	Impact energy [KJ/m^2]
1	0	180	38	26
2	4	180	47.1	23.6
3	0	240	34.6	30
4	4	240	42.8	27.14
5	0	210	36.1	28.3
6	4	210	44.75	25.7
7	2	180	43.7	27.3
8	2	240	39.7	31.4
9	2	210	40.5	29.75
10	2	210	41	29.7
11	2	210	40	29.65
12	2	210	42	29.8
13	2	210	39.5	29.6

RESULTS AND DISCUSSION

Development of RSM models

RSM is the procedure for determining the relationship between various process parameters with the various machining criteria and exploring the effect of these process parameters on the coupled responses [15].

To study the effects of the process parameters on the responses as mentioned above on the tensile strength and impact energy, the second-order polynomial response surface mathematical model can be developed as follows:

$$Y = b_0 + \sum_{i=1}^{k} b_i X_{iu} + \sum_{i=1}^{k} b_{ii} X_{iu}^2 + \sum_{i=1}^{k} b_{ij} X_{iu} X_{ju} \quad (1)$$

where Y is the response (tensile strength and impact energy); b_0, b_i, b_{ii}, *and* b_{ij} are the coefficients; X_{iu} is the variable (W and T); u is the experiment number (1-13); k is the factor number (1-2); X_{iu}^2 is the higher-order term of the variable and X_{iu}, X_{ju} are the interaction terms.

Based on equation (1), the effects of the process variables mentioned above on the magnitude of the tensile strength and impact energy were evaluated by computing the values of the different constants of Eq. (1) using the indigenously-developed computer software MINITAB and utilizing the relevant data from Table 2.

The mathematical relationships for correlating the mentioned responses are presented in equations (2) and (3):

$$TS\,[\text{MPa}] = 58 + 4W - 0.15T - 3.7\times10^{-3}WT + \\ -0.26W^2 + 2.2\times10^{-4}T^2 \quad (2)$$

For the impact energy

$$E\,[\text{KJ/m}^2] = -3.63 + 2.45W + 0.23T + \\ -1.9\times10^{-3}WT - 0.67W^2 - 4\times10^{-4}T^2 \quad (3)$$

In this work, analysis of variance (ANOVA) is used to verify the adequacy of the developed empirical relationships. The responses, namely, the tensile strength and impact energy, are presented in Tables 3 and 4, respectively. In this study, the model F-value and the associated probability values (P-value) are verified to confirm the significance of the empirical relationships. Furthermore, using the F-values the predominant factors which have major and minor effects on the responses could be assessed. The F-value assessment found that the predominant factors that directly influence the responses as per hierarchy are the silica content for the tensile strength and extrusion temperature for the impact energy.

The determination coefficient (R^2) indicates the goodness of fit for the model. In all the cases, the value of the determination coefficient ($R^2 > 0.99$) indicates that the empirical relationships do not explain less than 1% of the total variations.

The value of the adjusted determination coefficient is also high, which indicates the high significance of the empirical relationships. The predicted R^2 values also show good agreement with the adjusted R^2 values. Adequate precision compares the range of the predicted values at the design points with the average prediction error.

Simultaneously, a relatively low value of the coefficient of variation indicates the improved precision and reliability of the conducted experiments. The values of probability > F in Tables 3 and 4 for the empirical relationships are less than 0.05, which indicates that the empirical relationships are significant [16].

TABLE 3. **ANOVA results for tensile strength**

Source	Sum of squares	Degrees of freedom	F-value	Prob > F
Model	138.58	5	25869	< 0.0001
W	112.23	1	104000	< 0.0001
T	22.82	1	21294	< 0.0001
$W \times T$	0.2	1	189	< 0.0001
W^2	3.19	1	2979	< 0.0001
T^2	0.11	1	103.11	< 0.0001
$R^2 = 0.9999$, $R^2_{Adjusted} = 0.9999$ and $R^2_{Predicted} = 0.9994$				

TABLE 4. **ANOVA results for impact energy**

Source	Sum of squares	Degrees of freedom	F-value Prob > F	Prob > F
Model	59.45	5	2001	< 0.0001
W	10.3	1	1733	< 0.0001
T	22.58	1	3801	< 0.0001
$W \times T$	0.053	1	8.91	< 0.0001
W^2	20.027	1	3411	< 0.0001
T^2	0.36	1	59.91	< 0.0001
$R^2 = 0.9993$, $R^2_{Adjusted} = 0.9988$ and $R^2_{Predicted} = 0.9932$				

Figure 3 shows the comparison between the measured values of the response and those predicted by the RSM models. It is seen from the figure that good agreement exists between the two values. Hence, it can be inferred that the developed RSM models can predict the variation in tensile strength and impact energy against the variation in the process factors.

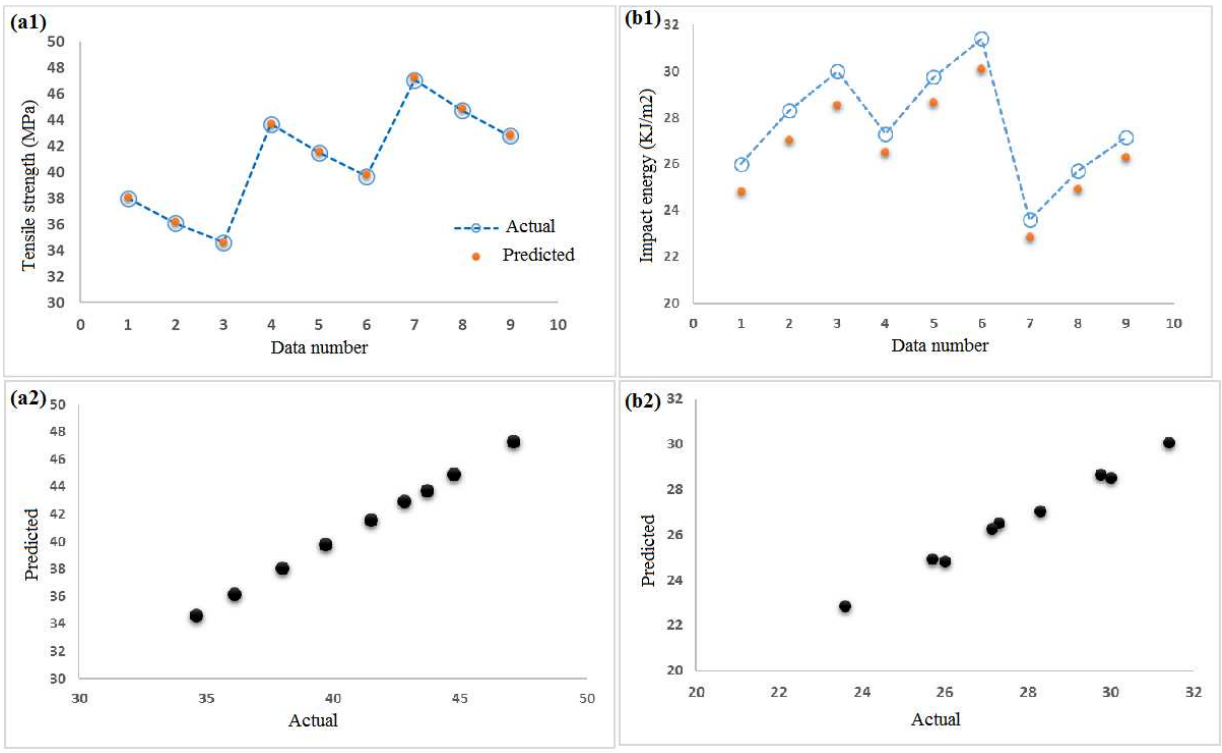

Fig. 3. Comparison of measured and predicted values for: a) tensile strength, b) impact energy

Parametric influence of tensile strength

After ascertaining the effect of the SiO_2 content on the tensile strength behavior of the fabricated composite, the parameter is varied over a 0 to 4 wt.% content while the temperature was kept constant at 210ºC. Figure 4a illustrates the influence of the silica content on the tensile strength of the fabricated composite. It is seen from the Figure that the tensile strength rises as the value of silica content increases.

When a ceramic phase like nanosilica is mixed with a polymeric material, the porosity in the cross-section of the fabricated composite is significantly reduced. In such conditions, the strength of the composite increases. On the other hand, in the study carried out by Ding et al. [17], they revealed that an augmentation in the ceramic phase content causes an increase in the elasticity modulus of the composite. Thus, the fabricated composite can endure a higher force, and the tensile strength increases.

Figure 5 presents the SEM micrograph that was obtained from the composite cross-section. It can be seen from the figure that an increase in the values of the silica content causes a reduction in the porosity, and the number of voids is reduced by adding silica. Therefore, a denser morphology results in a higher tensile strength. What is more, from Figure 4b it can be ascertained that an increase in the melt temperature during extrusion causes a decrease in the tensile strength values. During the extrusion process, when the extrusion temperature increases, the sensitivity of the material to degradation also increases, causing the formation of porosity in the morphology of the samples, which adversely affects the tensile strength of the composite.

Moreover, decreasing the melt viscosity causes air bubbles to form in the composite structure. In such conditions, the degree of porosity also rises and causes a reduction in the tensile strength.

Figure 6 illustrates the morphology of the cross-section of the fabricated composite. It is seen from the figure that increasing the number and dimensions of the voids in the composite is caused by a rise in the melt temperature. In such conditions the tensile strength decreases correspondingly.

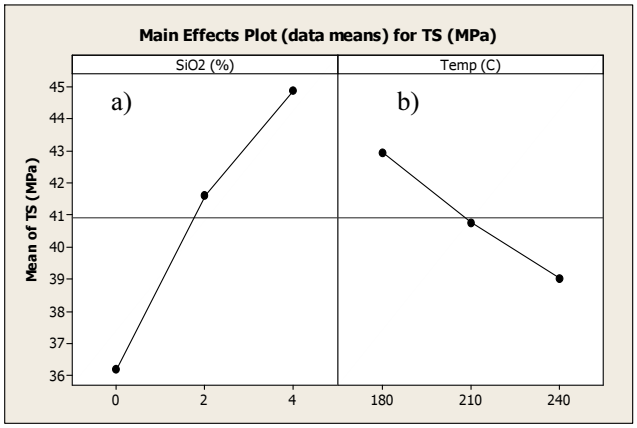

Fig. 4. Parametric influence of tensile strength: a) silica content, b) temperature

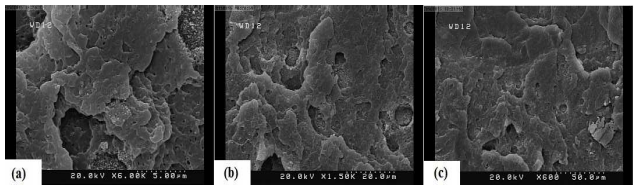

Fig. 5. Morphology of composite cross-sections with different silica contents: a) 0%, b) 2%, c) 4%

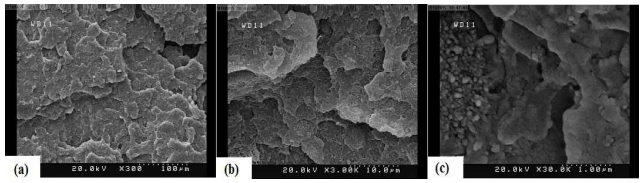

Fig. 6. Morphology of composite cross-sections produced under different temperatures: a) 180ºC, b) 210ºC, c) 240ºC

Figure 7a-c illustrates the interaction effects of the silica content and extrusion temperature on the tensile strength of the composite. To achieve a higher tensile strength, the silica content of 4%, and temperature of 180ºC should be selected. This trend is observed in all the figures, including the line plot, contour plot, and 3D surface plot.

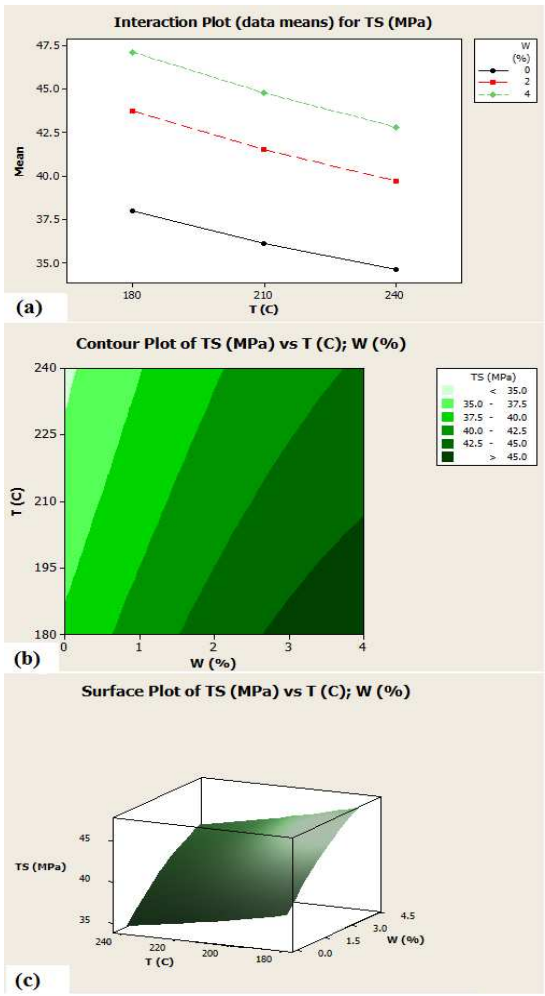

Fig. 7. Interaction effect of silica content and extrusion temperature on tensile strength of composite: a) line plot, b) contour plot, c) 3D surface plot

Parametric influence of impact energy

Figure 8 illustrates the effect of the production parameters on the impact energy of the fabricated composite. It can be observed in Figure 8b that an increase in the silica content causes first a rise in the impact energy at 2% and a reduction at 4%. It is worth mentioning that the impact energy is significantly affected by the ductility and brittleness of the fabricated composite. A higher value of ductility results in a higher impact strength and vice versa.

The stress-strain curves of the fabricated composite with different silica contents are presented in Figure 9a It is seen from the Figure that increases in the silica content result in a higher strength and lower elongation in the stress-strain curve. Therefore, in such conditions at a 2% silica content, the enhancement of the impact energy is due to the higher strength that results in a greater surface area in the stress-strain curve. Nevertheless, it was found that a further augmentation in the silica content changes the material behavior from ductile to brittle with a lower surface area under the curve. An increase in the silica content causes a decline in the impact energy. This comes from the fact that adding more silica makes the material more brittle.

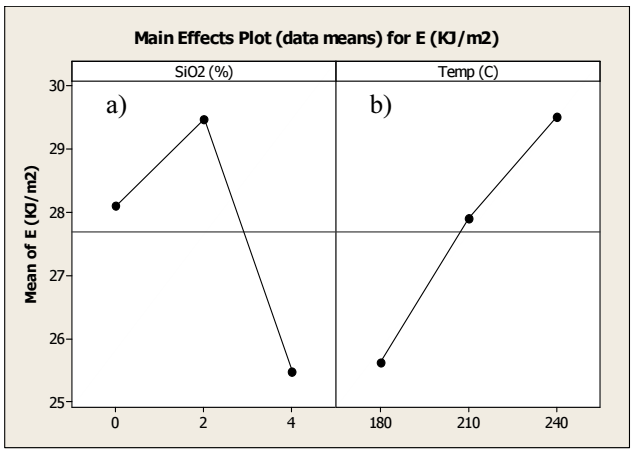

Fig. 8. Parametric influence of impact energy: a) silica content, b) temperature

From Figure 8b, it can be inferred that an increase in the extrusion temperature results in a higher impact energy. The stress-strain curve of the fabricated samples under different extrusion temperatures is presented in Figure 9b. It can be observed from the Figure that as the die temperature increases, the elongation of the fabricated samples increases while the stress decreases. This behavior represents a ductile type of material with a higher fracture toughness than a brittle material. In such conditions, the impact energy increases.

On the other hand, from Figure 9b it can be seen that the surface area under the curves for the temperature of 240ºC is relatively higher than the composites fabricated at 180 and 210ºC. Therefore, the impact energy of the composite increases owing to a rise in the extrusion temperature.

Figure 9a-c presents the interaction effects of the silica content and extrusion temperature on the impact energy of the fabricated composite. The silica content of 2% and temperature of 240ºC should be selected for to achieve the maximum impact energy. This trend is observed in all the figures, including the line plot, contour plot, and 3D surface plot.

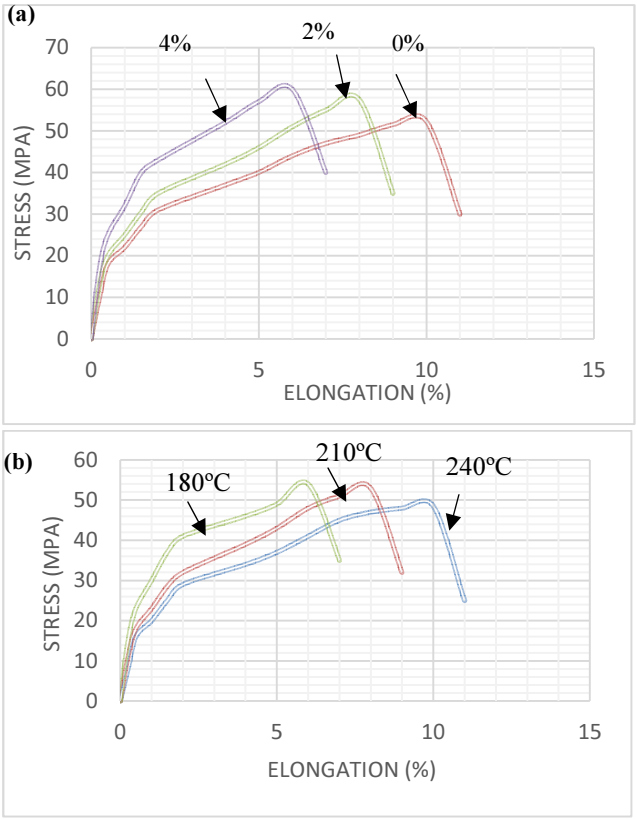

Fig. 9. Stress-strain curves of fabricated composite: a) regarding silica content, b) regarding temperature

Optimization

There are many statistical techniques for solving multiple response problems like overlaying the contour plots for each response, constrained optimization problems, and the desirability approach.

The desirability method is recommended due to its simplicity, availability of software, as well as flexibility in weighing and giving importance to individual responses. Solving such multiple-response optimization problems using this technique involves combining multiple responses into a dimensionless measure of performance called the overall desirability function [18].

The desirability of each response was calculated using Equations (4) and (6) in the present work. The shape of the desirability function can be changed for each goal by weight field w_i. Weights are used to emphasize the upper/lower bounds or emphasize the target value. The weights could range between 0.1 and 1; a weight greater than 1 places more emphasis on the aim, while weights less than 1 place less emphasis. When the weight value is equal to 1, it varies from 0 to 1 in a linear mode [17].

In the desirability objective function (D), each response can be assigned an importance (r), relative to the other responses. The importance varies from the least significant value of 1 to the most critical value of 5. If the varying degrees of importance are assigned to the different responses, the overall objective function is shown in Eq. (6) below, where n is the number of responses in the measure and r_i is the target value of the ith response.

The maximum desirability is defined by

$$d_i = \begin{cases} 0 & Y_i < Low_i \\ \left(\dfrac{Y_i - Low_i}{High_i - Low_i}\right)^w & Low_i < Y_i < High_i \\ 1 & Y_i > High_i \end{cases} \quad (4)$$

The minimum desirability is defined by:

$$d_i = \begin{cases} 1 & Y_i < Low_i \\ \left(\dfrac{Y_i - Low_i}{High_i - Low_i}\right)^w & Low_i < Y_i < High_i \\ 0 & Y_i > High_i \end{cases} \quad (5)$$

$$D = \left(\prod_{i=1}^{n} d_i^{r_i}\right)^{1/\sum r_i} \quad (6)$$

According to this technique, the desirability function can find one point or more for numerical optimization of the process.

The desirability function would satisfy all the responses with high or low requirements and search for optimum experimental conditions for mixing performance. The ultimate goal is to produce the maximum tensile strength (TS) and low weight ratio (WR), simultaneously. MINITAB software packages are utilized to determine the optimal experiment conditions.

To perform multi-characteristic optimization by the desirability approach, firstly, the optimization criteria should be identified. Table 5 presents the defined criterion for optimization, while Table 6 and Figure 10 present the optimal solutions based on the identified criterion.

TABLE 6. **Optimization criterion**

Factors/responses	Criterion	Importance
Silica content [%]	In range of 800-1600	-
Melt temperature [ºC]	In range of 40-80	-
Tensile strength [MPa]	Maximize	*****(5)
Impact energy [KJ/m^2]	Minimize	***** (5)

TABLE 7. **Optimal results as obtained by Design Expert based on identified criterion**

W [%]	T [ºC]	TS [MPa]	E [KJ/m^2]	Desirability [%]
1.87	198	42	29	100

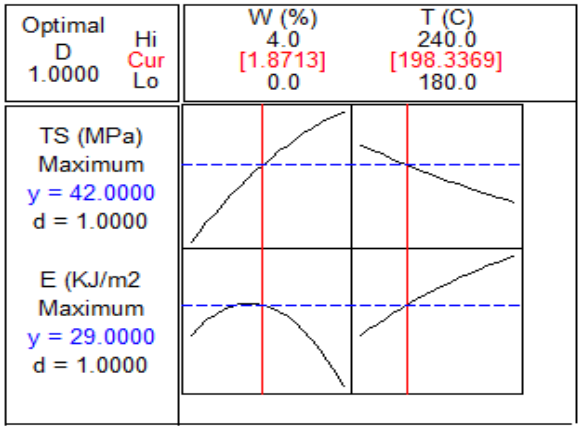

Fig. 10. Response optimizer plot showing optimum parameter combination for single objective and multi-objective optimization criteria

According to the results in Table 7 and Figure 10 it can be inferred that the silica content of 2% and temperature of 200ºC result in the maximum tensile strength and impact energy, simultaneously.

This parameter setting is completely logically based on what was discussed previously. It is seen from Figure 10 that with a 2% silica content and temperature of 200ºC, both the responses have desirable values with a desirability degree of 100%.

In order to approve the obtained optimal results, a confirmatory experiment was carried out using the obtained optimal parameters, and the results of the tensile strength and impact energy obtained from the confirmatory experiment were compared with those derived from the optimization approach.

Table 8 presents the comparison between the optimal results. It is ascertained from the results that good agreement exists between the results of the confirmatory experiment. The error values for both the predicted responses was below 10%, showing the accuracy and predictability of the proposed approach.

It can be inferred from the results that the proposed methodology could be effectively used to model and optimize the extrusion process in the fabrication of polymeric-based matrix nanocomposite.

Mechanical defects were made to the samples to analyze how the defects affect the mechanical strength of the composite. Figure 11 illustrates the effect of defects on the fatigue behavior. According to the Figure, both the tensile strength and impact energy of the fabricated samples with defects are about 30 and 50% lower than those of perfect samples.

Due to the high strain rate loading in the impact test, the propagated crack instantaneously causes a greater reduction in the mechanical strength during impact testing.

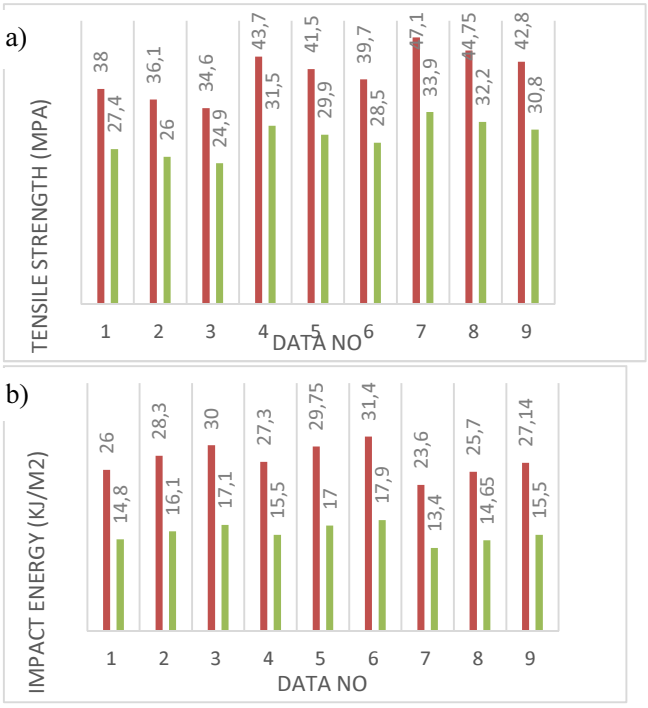

Fig. 11. Comparison of tensile strength (a), impact energy (b) of fabricated composite for perfect and defective samples

TABLE 8. **Results of confirmatory experiment**

Optimal setting		**TS [MPa]**	**E [KJ/m^2]**		
W [%]	T [ºC]	Prediction	Experiment	Prediction	Experiment
2	200	42	39.2	29	27.8

CONCLUSIONS

In the present work an experimental study was carried out to prepare an acrylonitrile-butadiene-styrene matrix composite reinforced by nanosilica particles. A twin extruder was utilized to fabricate the composite specimens prepared for tensile and impact tests. The experiments were carried out based on response surface methodology to identify the effect of the silica content and extrusion temperature on the tensile and impact strength.

The obtained results can be summarized as follows:

1. It was found from the results that an increase in silica content causes an increase in tensile strength, while a rise in the melt temperature results in a lower tensile strength. Consolidation due to the silica content was the primary mechanism of strengthening, and porosity due to high temperature was the main reason for strength reduction.
2. It was found that an increase in the silica content up to 2% augments the impact strength owing to the higher tensile strength, while a further increase in the silica content reduces the impact strength due to a decline in ductility.
3. A rise in the melt temperature causes an increase in ductility and in turn enhances the elongation at break. In such conditions, the impact energy increases and enhances the fracture toughness.
4. The optimization results revealed that for a simultaneous achievement of the maximum tensile strength and impact energy, the silica content of 2% and temperature of 200ºC should be selected. In these conditions, a tensile strength of 42 MPa and an impact energy of 29.2 KJ/m^2 were attained. The desirability of the results at under these conditions was about 100%.

REFERENCES

[1] Bohatka T., Moet A., The effect of load level on the mechanism of fatigue crack propagation in ABS, Journal of Materials Science 1995, 30(18), 4676-4683.

[2] Li Q., Tian M., Kim D., Zhang L., Jin R., Compatibility and thermal properties of poly (acrylonitrile-butadiene-styrene) copolymer blends with poly (methyl methacrylate) and poly (styrene-co-acrylonitrile), Journal of Applied Polymer Science 2002, 85(13), 2652-2660.

[3] Zheng K., Chen L., Li Y., Cui P., Preparation and thermal properties of silica-graft acrylonitrile-butadiene-styrene nanocomposites, Polymer Engineering & Science 2004, 44(6), 1077-1082.

[4] Jang L.W., Kang C.M., Lee D.C., A new hybrid nanocomposite prepared by emulsion copolymerization of ABS in the presence of clay, Journal of Polymer Science Part B: Polymer Physics 2001, 39(6), 719-727.

[5] Wang S., Hu Y., Song L., Wang Z., Chen Z., Fan W., Preparation and thermal properties of ABS/montmorillonite nanocomposite, Polymer Degradation and Stability 2002, 77(3), 423-426.

[6] Stretz H., Paul D., Cassidy P., Poly (styrene-co-acrylonitrile)/ montmorillonite organoclay mixtures: a model system for ABS nanocomposites, Polymer 2005, 46(11), 3818-3830.

[7] Pourabas B., Raeesi V., Preparation of ABS/montmorillonite nanocomposite using a solvent/non-solvent method, Polymer 2005, 46(15), 5533-5540.

[8] Jang B.N., Wilkie C.A., The effects of clay on the thermal degradation behavior of poly (styrene-co-acrylonitirile), Polymer 2005, 46(23), 9702-9713.

[9] Modesti M., Besco S., Lorenzetti A., Causin V., Marega C., Gilman J., Fox D., Trulove P., De Long H., Zammarano M., ABS/clay nanocomposites obtained by a solution technique: Influence of clay organic modifiers, Polymer Degradation and Stability 2007, 92(12), 2206-2213.

[10] Teng X., Liu H., Huang C., Effect of Al_2O_3 particle size on the mechanical properties of alumina-based ceramics, Materials Science and Engineering: A 2007, 452, 545-551.

[11] Kuo M., Tsai C., Huang J., Chen M., PEEK composites reinforced by nano-sized SiO_2 and Al_2O_3 particulates, Materials Chemistry and Physics 2005, 90(1), 185-195.

[12] Lin Q., Yang G., Liu J., Application and mechanism principium research on nano-SiO_2/urea formaldehyde resin, Journal of Fujian College of Forestry 2005, 2.

[13] Devi R.R., Maji T.K., Effect of nano-SiO_2 on properties of wood/polymer/clay nanocomposites, Wood Science and Technology 2012, 46(6), 1151-1168.

[14] Hsu Y.G., Lin F.J., Organic-inorganic composite materials from acrylonitrile-butadiene-styrene copolymers (ABS) and silica through an in situ sol-gel process, Journal of Applied Polymer Science 2000, 75(2), 275-283.

[15] Myers R.H., Montgomery D.C., Anderson-Cook C.M., Response Surface Methodology: Process and Product Optimization Using Designed Experiments, John Wiley & Sons, 2016.

[16] Rajakumar S., Muralidharan C., Balasubramanian V., Response surfaces and sensitivity analysis for friction stir welded AA6061-T6 aluminium alloy joints, International Journal of Manufacturing Research 2011, 6(3), 215-235.

[17] Ding C., Jia D., He H., Guo B., Hong H., How organo-montmorillonite truly affects the structure and properties of polypropylene, Polymer Testing 2005, 24(1), 94-100.

[18] Rajakumar S., Muralidharan C., Balasubramanian V., Predicting tensile strength, hardness and corrosion rate of friction stir welded AA6061-T 6 aluminium alloy joints, Materials & Design 2011, 32(5), 2878-2890.

